Testing of the Programmable AMB Spring and Damping Forces in a Flexible Rotor Test-Rig Mode

Adam Piłat[1,a]
[1]AGH University of Science and Technology, Department of Automatics,
Mickiewicza 30 Ave, 30-059 Kraków, Poland
[a]ap@agh.edu.pl

Abstract: This paper presents the 3 coils Active Magnetic Bearing (AMB) applied to the spring and damping forces generation in the flexible rotor mode. A nonlinear model is linearized for the rotor located at the bearing center. A state feedback controller is proposed and a closed loop matrix is given in the final form. Stiffness and damping factors are adjusted for experimental purposes to show effects of the programmable advantages of the AMB. The experimental results illustrate the damped rotor vibrations under an external pulse excitation generated by one of electromagnets.

Keywords: Stiffness, Damping, Active Magnetic Bearing, Real-Time Control, Programmable Dynamics

Introduction

Apart from some operating rotational speed, the rotor can-not be considered as a rigid body but as a flexible one [1, 2]. Also long sets of rotating shafts ought to be considered as flexible rotors [8, 10]. A designed configurable laboratory test-rig was developed to observe a flexible rotor behaviour and to test the AMB stabilizing controller. A 3D model of the rotor has been prepared for the Finite Element Method analysis. A simulation stage illustrates the bending mode of the rotor. Figure 1 presents configuration of the system for this research and the numerical simulation of the first eigen frequency. The flexible rotor is modelled in a modified form of the Jeffcot rotor assuming 2DOFs, rotor stiffness and damping coefficients as well as fixed velocity. The static displacement is observed in a steady state due to the concentrated rotor part dedicated to the AMB operation – see Fig. 1c.

In order to test a wide range of rotating machines configurations in the laboratory area, the scaled and reconfigurable system was designed (see Fig. 1b). The mechanical elements, electronic circuits, control architecture and software can be set in many ways to realize a wide range of research tasks. The designed laboratory system consists of the following elements: 1-a mounting support with vibration isolation washer, 2-a ball bearings, 3-an active magnetic bearing, 4-a drive, 5-a clutch, 6-an unbalance disk, 8-a flexible rotor (see Fig. 1a). They can be configured in a various ways. .

The active magnetic bearing technology makes enables to control a hazardous level of rotor vibrations in transient states of the machine operation [5, 7, 9]. In a machine with the flexible rotor the critical speed can be observed. To eliminate rotor vibrations the AMB with programmable feedback is used. The aim of the control algorithm is to protect the rotor against damage by vibrations damping. A wide range of control algorithms can be used in this mode. In this paper, a state feedback controller with programmable stiffness and damping is proposed and tested in the levitation mode without rotations.

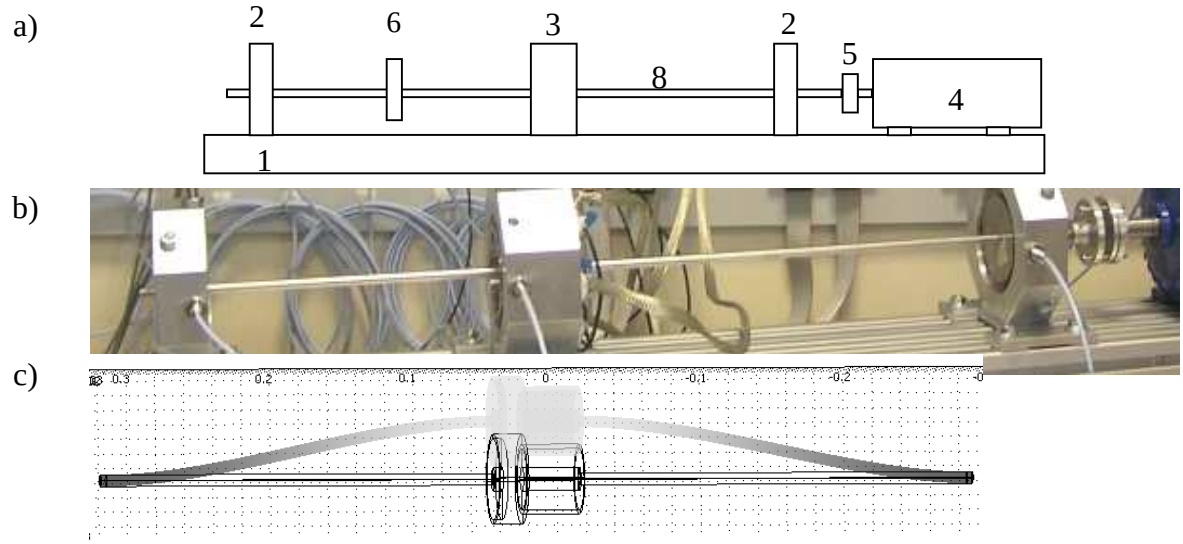

Fig. 1. Flexible rotor test-rig: a) configuration, b) laboratory-set-up, c) modelling eigen frequencies - view of the first mode.

Modelling

The presented laboratory test-rig can be considered as a typical Jeffcot rotor and modelled with the use of general equation (1) assuming point mass m, stiffness k_x, k_y and damping c_x, c_y of mechanical parts, rotor eccentricity e and constant rotational speed ω.

$$\begin{aligned} f_x(t) &= -k_x \cdot x - c_x \cdot \dot{x} - m \cdot \ddot{x} + m \cdot \omega^2 \cdot e \cdot \cos(2\pi\omega t + \varphi(t_0)) \\ f_y(t) &= -k_y \cdot y - c_y \cdot \dot{y} - m \cdot \ddot{y} + m \cdot \omega^2 \cdot e \cdot \sin(2\pi\omega t + \varphi(t_0)) \end{aligned} \tag{1}$$

The heteropolar 3 coils AMB is installed in the test rig for control purposes. A configuration of the rotor located at the bearing plane is presented in Fig. 2. There are three forces distributed at every 120 degrees and affecting the rotor. Three electromagnetic forces acting on the rotor are generated by two electromagnets located at the top of the AMB while the third one is placed at the bottom and its force acts with gravity force. Such configuration allows an optimal compensation of the inertia load. The calculation of local levitation gaps is performed on the basis of two eddy-current probe measurements located in a sensor plane and distributed one to another at 90 degrees.

Working in the gravity field and inserting the rotor disk into the 3 coils AMB the equation (1) is extended to the nonlinear form (2).

$$\begin{aligned} f_x(t) = &-k_x \cdot x - c_x \cdot \dot{x} - m \cdot \ddot{x} + F_{e1} \cdot \cos(\alpha_1) + F_{e2} \cdot \cos(\alpha_2) + \\ &F_{e3} \cdot \cos(\alpha_3) + m \cdot \omega^2 \cdot e \cdot \cos(2\pi\omega t + \varphi(t_0)) \\ f_y(t) = &-k_y \cdot y - c_y \cdot \dot{y} - m \cdot \ddot{y} - m \cdot g + F_{e1} \cdot \sin(\alpha_1) + F_{e2} \cdot \sin(\alpha_2) + \\ &F_{e3} \cdot \sin(\alpha_3) + m \cdot \omega^2 \cdot e \cdot \sin(2\pi\omega t + \varphi(t_0)) \end{aligned} \tag{2}$$

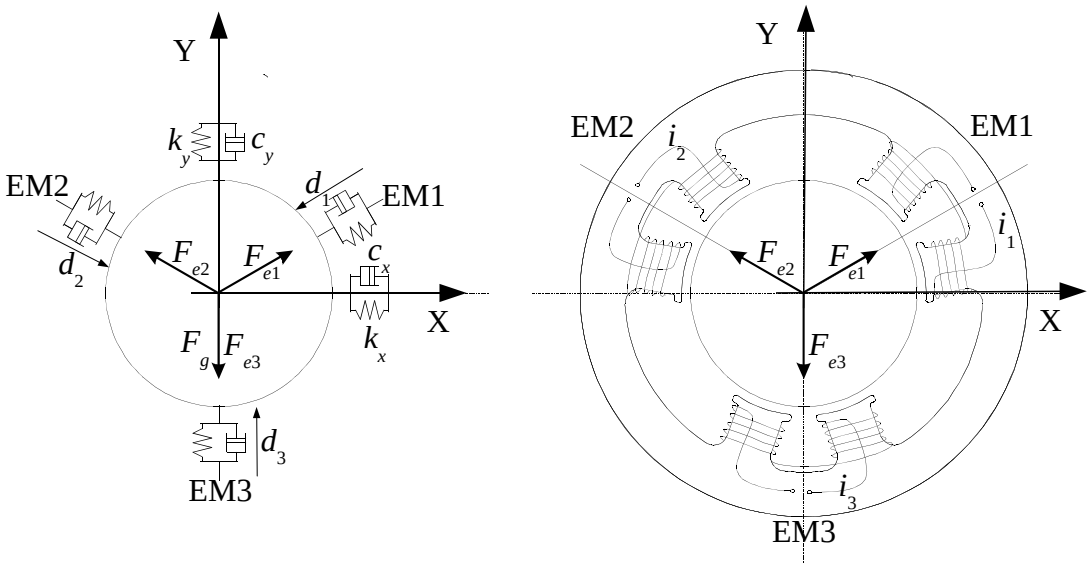

Fig. 2. Configuration of the AMB and electromagnetic forces acting on the rotor.

Assuming that the electromagnetic force is modelled by electromagnet constant K_e, coil current i and distance d between rotor and AMB poles formula (2) is rewritten to the form (3)

$$\begin{aligned}\ddot{x} &= -\frac{k_x \cdot x}{m} - \frac{c_x \cdot \dot{x}}{m} + \frac{\sqrt{3}}{2} \cdot \frac{K_{e1} \cdot i_1^2}{d_1^2 \cdot m} - \frac{\sqrt{3}}{2} \cdot \frac{K_{e2} \cdot i_2^2}{d_2^2 \cdot m} + \omega^2 \cdot e \cdot \cos(2\pi\omega t + \varphi(t_0)) \\ \ddot{y} &= -\frac{k_y \cdot y}{m} - \frac{c_y \cdot \dot{y}}{m} - g + \frac{1}{2} \cdot \frac{K_{e1} \cdot i_1^2}{d_1^2 \cdot m} + \frac{1}{2} \cdot \frac{K_{e2} \cdot i_2^2}{d_2^2 \cdot m} - \frac{K_{e3} \cdot i_3^2}{d_3^2 \cdot m} + \omega^2 \cdot e \cdot \sin(2\pi\omega t + \varphi(t_0))\end{aligned} \tag{3}$$

Because of the AMB construction and actuators location the steady-state current for the rotor located at the bearing center (0,0) depending on the gravity force and user-defined AMB action force P are calculated as follows:

$$i_{100} = \sqrt{\frac{d_{100}^2 \cdot (m \cdot g + P)}{K_{e1}}} \qquad i_{200} = \sqrt{\frac{d_{200}^2 \cdot (m \cdot g + P)}{K_{e2}}} \qquad i_{300} = \sqrt{\frac{d_{300}^2 \cdot P}{K_{e3}}} \tag{4}$$

For the linear controller design the nonlinear system (3) is linearized for the rotor located at the bearing center and steady-state coil currents. Introducing the state vector $x=col\{x_1, x_2, x_3, x_4\}$ corresponding to the displacement and velocity in X and Y axis respectively, the linear model is given in the following form (6).

$$\begin{aligned}\dot{x} &= A_o \cdot x + B \cdot u \\ y &= C \cdot x\end{aligned} \tag{5}$$

The control signal is represented by the current driving the coil and it is assumed that the velocity is retrieved from position signals.

$$u = \begin{bmatrix} i_1 - i_{100} \\ i_2 - i_{200} \\ i_3 - i_{300} \end{bmatrix} \tag{6}$$

The state and control matrices are calculated as follows:

$$A_o = \begin{bmatrix} 0 & 1 & 0 & 0 \\ a_{21} & a_{22} & a_{23} & 0 \\ 0 & 0 & 0 & 1 \\ a_{41} & 0 & a_{43} & a_{44} \end{bmatrix} \qquad B = \begin{bmatrix} 0 & 0 & 0 \\ b_{21} & b_{22} & 0 \\ 0 & 0 & 0 \\ b_{41} & b_{42} & b_{43} \end{bmatrix} \tag{7}$$

The state and control matrices coefficients are calculated by (8), (9) and (10).

$$\begin{aligned} a_{21} &= -\frac{k_x}{m} - \frac{\sqrt{3}\cdot K_{e1}\cdot i_{100}^2}{d_{100}^3\cdot m}\cdot\frac{\partial d_1}{\partial x_1} + \frac{\sqrt{3}\cdot K_{e2}\cdot i_{200}^2}{d_{200}^3\cdot m}\cdot\frac{\partial d_2}{\partial x_1} \\ a_{22} &= -\frac{c_x}{m} \\ a_{23} &= -\frac{\sqrt{3}\cdot K_{e1}\cdot i_{100}^2}{d_{100}^3\cdot m}\cdot\frac{\partial d_1}{\partial x_3} + \frac{\sqrt{3}\cdot K_{e2}\cdot i_{200}^2}{d_{200}^3\cdot m}\cdot\frac{\partial d_2}{\partial x_3} \end{aligned} \tag{8}$$

$$\begin{aligned} a_{41} &= -\frac{K_{e1}\cdot i_{100}^2}{d_{100}^3\cdot m}\cdot\frac{\partial d_1}{\partial x_1} - \frac{K_{e2}\cdot i_{200}^2}{d_{200}^3\cdot m}\cdot\frac{\partial d_2}{\partial x_1} + \frac{2\cdot K_{e3}\cdot i_{300}^2}{d_{300}^3\cdot m}\cdot\frac{\partial d_3}{\partial x_1} \\ a_{43} &= -\frac{k_y}{m} - \frac{K_{e1}\cdot i_{100}^2}{d_{100}^3\cdot m}\cdot\frac{\partial d_1}{\partial x_3} - \frac{K_{e2}\cdot i_{200}^2}{d_{200}^3\cdot m}\cdot\frac{\partial d_2}{\partial x_3} + \frac{2\cdot K_{e3}\cdot i_{300}^2}{d_{300}^3\cdot m}\cdot\frac{\partial d_3}{\partial x_3} \\ a_{44} &= -\frac{c_y}{m} \end{aligned} \tag{9}$$

$$\begin{aligned} b_{21} &= \frac{\sqrt{3}\cdot K_{e1}\cdot i_{100}}{d_{100}^2\cdot m} \qquad b_{22} = -\frac{\sqrt{3}\cdot K_{e2}\cdot i_{200}}{d_{200}^2\cdot m} \\ b_{41} &= \frac{K_{e1}\cdot i_{100}}{d_{100}^2\cdot m} \qquad b_{42} = \frac{K_{e2}\cdot i_{200}}{d_{200}^2\cdot m} \qquad b_{43} = -\frac{2\cdot K_{e3}\cdot i_{300}}{d_{300}^2\cdot m} \end{aligned} \tag{10}$$

The proposed state feedback controller $u = -Kx$ is given in the form of (12) resulting in a closed loop system $A_c = A_o - BK$.

$$K = \begin{bmatrix} k_{11} & k_{12} & k_{13} & k_{14} \\ -k_{11} & -k_{12} & k_{13} & k_{14} \\ 0 & 0 & k_{33} & k_{34} \end{bmatrix} \tag{12}$$

One can find out that the elements a_{21} and a_{43} contain the rotor stiffness and the elements

a_{22} and a_{44} represents the rotor damping. The control signals are generated for all three axes. Observing a small influence of a_{23} and a_{41} components with respect to others in the matrix A_o, and analyzing the form of control matrix B where two pairs b_{12}, b_{22} and b_{41}, b_{42} have the same values in pairs but opposite signs, the closed loop matrix A_c is given in the form of (13).

$$A_c = \begin{bmatrix} 0 & 1 & 0 & 0 \\ ac_{21} & ac_{22} & 0 & 0 \\ 0 & 0 & 0 & 1 \\ 0 & 0 & ac_{43} & ac_{44} \end{bmatrix} \tag{13}$$

One can find out that the ac_{21} and ac_{22} correspond to the stiffness in *X* and *Y* axis while ac_{22} and ac_{44} correspond to the damping. Excluding the object mass and multiplying these coefficients by the state vector spring and damping forces in *X* an *Y* axes can be calculated. Assuming required performance the controller *K* (12) is calculated using (13) and the pole placement technique applied to levitation systems [4]. The comparison of designed controllers in a such way is in progress.

Experimental investigation

The stand alone PC with MATLAB/Simulink software is used to design and execute control strategy in the real-time using Real Time Windows Target. The signals flow between PC and AMB test-rig is provided by the home-made PCI control and data acquisition board [3]. The main advantage of this board is parallel data acquisition. This board is specially dedicated to interface MIMO systems because it is able to measure up to 16 analogue signals and control up to 4 analogue interfaces. The internal logic controls all converters in simultaneous mode thus time delay between samples is eliminated and quality of control tasks is significantly improved. The FPGA to PCI interface allows to communicate the software algorithms to exchange measured and control data with MATLAB/Simulink at 10kHz. The 0.552kg have the rotor placed at the center of 80cm long shaft and it is located in the AMB plane. Without control the rotor lies at the bottom electromagnet. There is no safety bearing installed. The radial air gap is equal to 400μm and the maximal coil current is 1.2A at 12V power supply. The aim of the experimental stage is to observe the performance of the designed controller. To do this the rotor is levitating in the bearing are and it is excited by the force pulse generated by the lower electromagnet using current pulse of 0.5A at time 0.51s activated for10ms. Depending on the adjusted spring and damping force values the response of the system varies and the rotor trajectory illustrates the closed loop properties (Figs. 3-5). The presented coil currents present the controller reaction on the pulse excitation.

Comparing obtained results one can find effects of increased spring and damping forces. The second experiment illustrates increased oscillations due to the high stiffness and low damping. For the highest stiffness value, the control system requirements of the sampling rate increases and the sampling frequency should be adjusted versus natural frequency of the no damped closed loop system. In the presented experiment the sampling frequency remained constant at 10kHz.

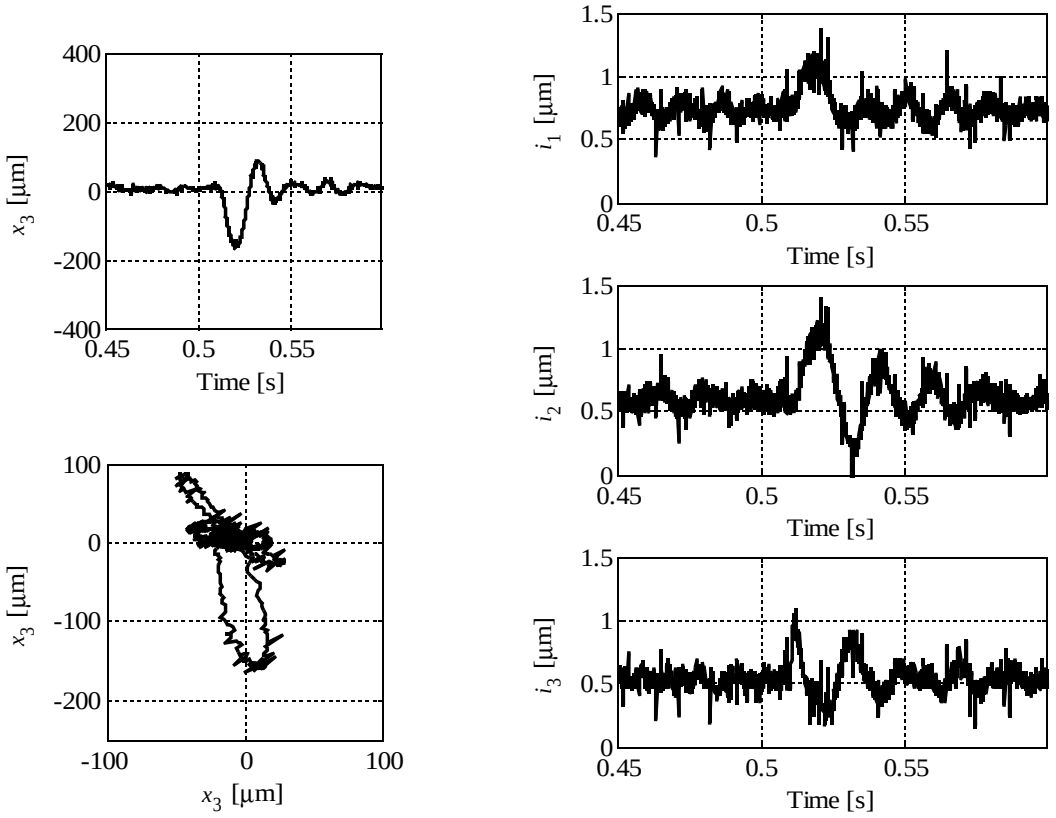

Fig. 3. Stiffness and damping factors equal to 552N/m and 2.76Ns/m respectively.

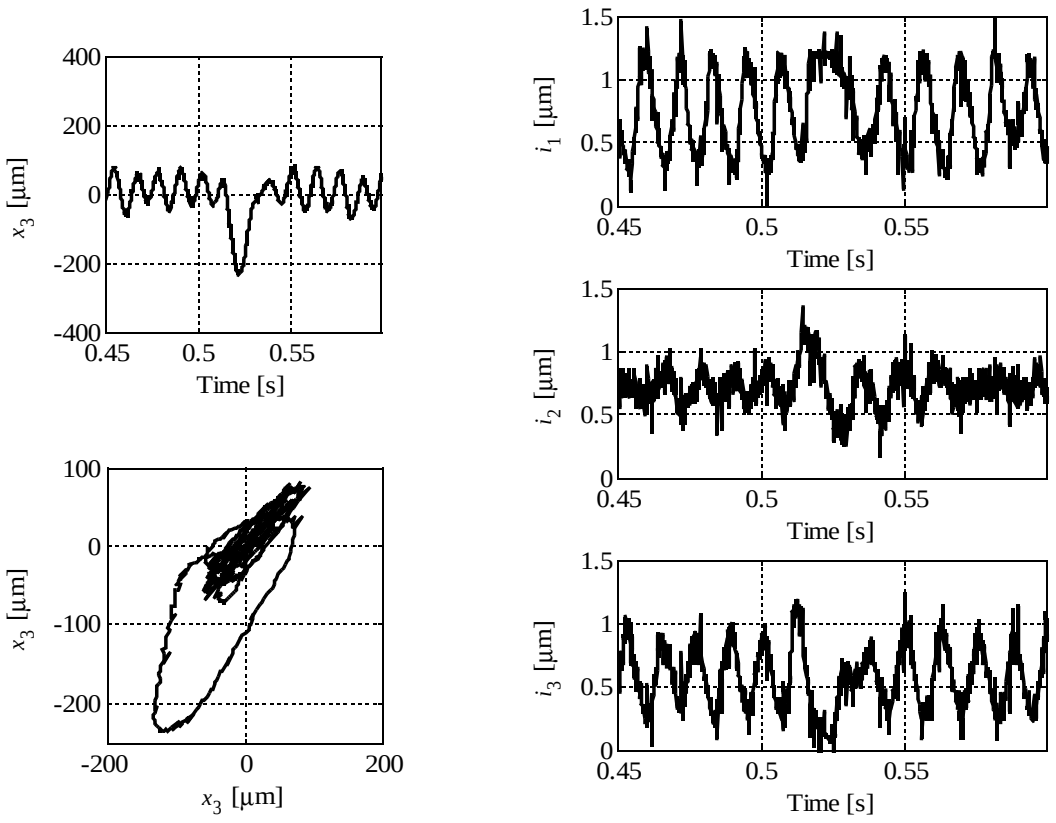

Fig. 4. Stiffness and damping factors equal to 16560N/m and 2.76Ns/m respectively.

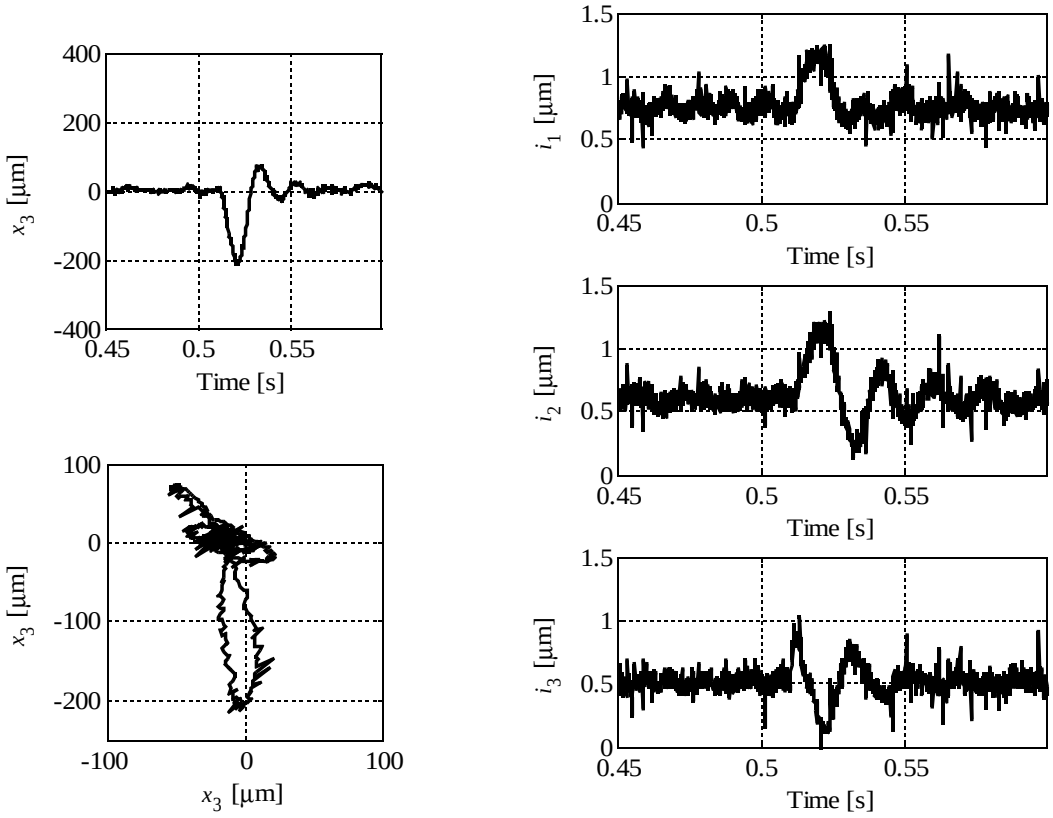

Fig. 5. Stiffness and damping factors equal to 16560N/m and 82.8Ns/m respectively.

Conclusions

The simplification of the model flexible rotor and the proposed controller has been fullfilled. The 3 coils current driven AMB was used for the rotor the stabilization and the bearing center. The programmed stiffness and damping factors make the construction applicable to the long shaft vibration damping and control of flexible rotor modes. The first experiments with the control of spring and damping forces confirm that it is possible to formulate the control law in a such way that appropriate parameters could represent precisely adjusted mechanical coefficients. These factors should be given together with current and displacement stiffness to characterize the AMB.

Acknowledgement

This research was supported by the Polish Scientific Research Grant No 3585/B/T02/2009/37

References

[1] Gosiewski Z., Muszyńska A.: Dynamics of rotating machinery. Wydawnictwo Uczelniane Wyższej Szkoły Inżynierskiej w Koszalinie, Koszalin 1992.
[2] Gryboś R. Dynamics of rotating machinery (in Polish), PWN, Warszawa 1994
[3] Piątek P., Piłat A., Multichannel control & measurement board with parallel data processing, Recent advances in control and automation, Warsaw, Academic Publishing House EXIT, 2008, pp. 373 ÷ 380
[4] Piłat A., Stiffness and damping analysis for pole placement method applied to active

magnetic suspension (in Polish), Automatyka, ISSN 1429-3447. 2009 vol. 13 no. 1 pp. 43-54

[5] Piłat A, Control of Magnetic Levitation Systems, Ph.D. Thesis (in Polish), AGH University of Science and Technology, Department of Automatics, Poland, Krakow 2002

[6] Piłat, A. & Grega W., Reconfigurable test-rig for AMB control, Proceedings of 7th Conference on Active Noise and Vibration Control Methods, pp. 1-8, June 2005, Wigry, Poland

[7] Proceedings of the International Symposium on Active Magnetic Bearings (1988-2006)

[8] Silva, Clarence de W., (2000), Vibration Fundamentals and Practice, CRC Press 2000.

[9] Schweitzer G., Maslen E.H. (Eds.), Magnetic Bearings, Theory, Design, and Application to Rotating Machinery, Springer, 2009.

[10] Wowk V.: Machinery Vibration, Measurement and Analysis. McGraw-Hill, Inc. 1991.